5-2000

Rotation-Invariant Synthetic Discriminant Function Filter for Pattern Recognition

Vahid R. Riasati
University of South Alabama

Partha P. Banerjee
University of Dayton, pbanerjee1@udayton.edu

Mustafa A. G. Abushagur
University of Alabama, Huntsville

Kenneth B. Howell
University of Alabama, Huntsville

Rotation-invariant synthetic discriminant function filter for pattern recognition

Vahid R. Riasati, MEMBER SPIE
University of South Alabama
Electrical and Computer Engineering Department
307 University Boulevard
Mobile, Alabama 36688-0002

Partha P. Banerjee, FELLOW SPIE
Mustafa A. G. Abushagur, MEMBER SPIE
University of Alabama in Huntsville
Electrical and Computer Engineering Department
Huntsville, Alabama 35899

Kenneth B. Howell
University of Alabama in Huntsville
Mathematics and Statistics Department
Huntsville, Alabama 35899

Abstract. The ring synthetic discriminant function (RSDF) filter for rotation-invariant response is discussed for pattern recognition. This method uses one half of a slice of the Fourier transform of the object to generate the transfer function of the filter. This is accomplished by rotating the one half of a slice in the Fourier domain through 2π rad about the zero-frequency point of the Fourier plane. This filter has the advantage of always matching at least one half of a slice of the Fourier transform of any rotation of the image. An analytical discussion of the filter construction and correlation results are presented along with simulated correlation results for a particular target image. These results and established metrics are used for comparison with benchmark algorithms. [S0091-3286(00)00505-5]

Subject terms: projection-slice filter; rotation-invariant filter; synthetic discriminant function; optical pattern recognition; ring filter.

Paper ATR-006 received Aug. 26, 1999; revised manuscript received Nov. 18, 1999; accepted for publication Dec. 10, 1999.

1 Rotation-Invariant Projection-Slice Synthetic Discriminant Function, Ring Filter

Images produced by computer-assisted tomography (CAT scans) and similar methods using magnetic resonance, sound waves, isotope emission, x-ray scattering, etc., all form projections from nondestructive probing of an object.[1–3] Since these projections represent particular features of the object, we used these projections for the synthesis of distortion-invariant filters.[4–6] There is a unique relationship between the projection of an object and the Fourier transform of that object. This relationship is formalized as the projection-slice theorem (PST). Since projections are strictly mathematical operations they can be formed in n-dimensional, n-D, space. Here, we are working in 2-D space. Given an image $s(x,y)$ with a 2-D Fourier transform (FT) $S(u,v)$, the FT of the projection of $s(x,y)$ is a slice of $S(u,v)$, taken at an angle θ, and is given by

$$S_\theta(\omega)=S(\omega\cos\theta,\omega\sin\theta), \tag{1}$$

where ω is the radian frequency, and $u=\omega\cos\theta$ and $v=\omega\sin\theta$ are the horizontal and vertical axes in the frequency domain. This is referred to as the 2-D PST.

Taking only a single slice of the FT of the image, Eq. (1) can be given by $S_{\theta_0}(\omega)=S(\omega\cos\theta_0,\omega\sin\theta_0)$, where θ is fixed at θ_0, with no *a priori* information about the object other than, perhaps, finite support and that it is real, a rotation-invariant filter can be constructed from one half of a 1-D Fourier domain slice of the object. This is done by rotating the half slice in the Fourier plane to generate a 2-D circular symmetric function $H(u,v)$ as the transfer function of the rotation invariant filter or ''ring filter.'' Thus, the transfer function of the rotation invariant filter $H(u,v)$ can be written as

$$H(u,v)=\alpha S(|\omega|\cos\theta_0,|\omega|\sin\theta_0)|\omega|^\gamma, \tag{2}$$

where α is a real multiplicative constant not equal to zero, and γ is a real and positive constant. Using Eq. (2) and the fact that only one half of a slice is used, the ring filter transfer function can also be given by

$$\begin{aligned}H(u,v)&=\alpha S_{\theta_0}(|\omega|)|\omega|^\gamma\\&=\alpha|S_{\theta_0}(\omega)||\omega|^\gamma\exp[j\psi(|\omega|)],\end{aligned} \tag{3}$$

where $\psi(\omega)$ is the phase angle associated with the particular slice of the frequency information used. In using Eq. (1) from the previous section, Eq. (3) makes the modification of using only a half of a slice rather than the full slice of the FT.

The impulse response of the ring filter $h(x,y)$ can be obtained from the transfer function $H(u,v)$ by means of the FT inversion integral:

$$h(x,y)=\frac{1}{4\pi^2}\int_{-\infty}^{\infty}\int_{-\infty}^{\infty}H(u,v)\exp[j(xu+yv)]\,du\,dv. \tag{4}$$

Substituting Eq. (3) into Eq. (4), and writing it in polar coordinates (ω,θ), the 2-D inverse FT can be written as

$$\begin{aligned}h(x,y)=\frac{\alpha}{4\pi^2}\int_{-\infty}^{\infty}\int_0^{\pi}&S_{\theta_0}(|\omega|)\\&\times\exp(jx\omega\cos\theta+jy\omega\sin\theta)|\omega|^{\gamma+1}\,d\theta\,d\omega.\end{aligned} \tag{5}$$

 0091-3286/2000/$15.00

Setting α equal to unity and using the following change of variables,

$$x=\rho\cos\varphi, \tag{6}$$

$$y=\rho\sin\varphi, \tag{7}$$

$$\rho=(x^2+y^2)^{1/2}, \tag{8}$$

and

$$\varphi=\tan^{-1}\left(\frac{y}{x}\right), \tag{9}$$

the impulse response of the filter can be given by

$$\begin{aligned} h(\rho\cos\varphi,\rho\sin\varphi)&=\frac{1}{4\pi^2}\int_0^{\infty}\int_0^{2\pi}S_{\theta_0}(\omega)\\ &\quad\times\exp\{j\rho\omega[\cos(\varphi-\theta)]\}\omega^{\gamma+1}\,\mathrm{d}\theta\,\mathrm{d}\omega\\ &=\frac{1}{4\pi^2}\int_0^{\infty}\int_0^{2\pi}S_{\theta_0}(\omega)\\ &\quad\times\exp\{j\rho\omega[\cos(\varphi-\theta)]\}\omega^{\gamma+1}\,\mathrm{d}\theta\,\mathrm{d}\omega\\ &=\frac{1}{2\pi}\int_0^{\infty}S_{\theta_0}(\omega)J_0(\rho\omega)\omega^{\gamma+1}\,\mathrm{d}\omega\\ &=B^{-1}[S_{\theta_0}(\omega)\omega^{\gamma+1}], \end{aligned} \tag{10}$$

where $J_0(\cdot)$ is the Bessel function of the first kind and zeroth order, and $B^{-1}(\cdot)$, represents the inverse Fourier Bessel transform[7] and results in a circularly symmetric impulse response for the ring filter.

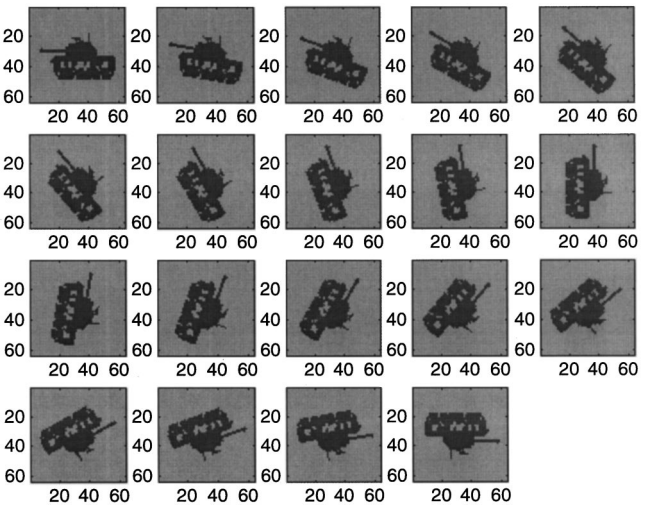

Fig. 1 The training images used for the implementation of the SDF filter. The top left corner image is the zero-degree rotated target, which is used to implement the MF as well as the ring filter.

2 Simulations

This section presents the results of the simulation efforts that are performed to generate the transfer function and impulse response of the ring filter. Here a one half slice of the 2-D FT of the image is used for $\omega\geqslant 0$, $\theta_0=0$, $\alpha=1$, and $\gamma=1$. The image is a generic tank shown in Fig. 1 along with 18 other images taken at increments of 10-deg in-plane rotation. The matched filter (MF) is implemented by the utilization of the undistorted target, and the synthetic discriminant function (SDF) filter is implemented by combining the 19 training images shown in Fig. 1.

The ring filter uses only the 0-deg image for its implementation. The transfer function and the impulse response of the ring filter are shown in Fig. 2; it is implemented by

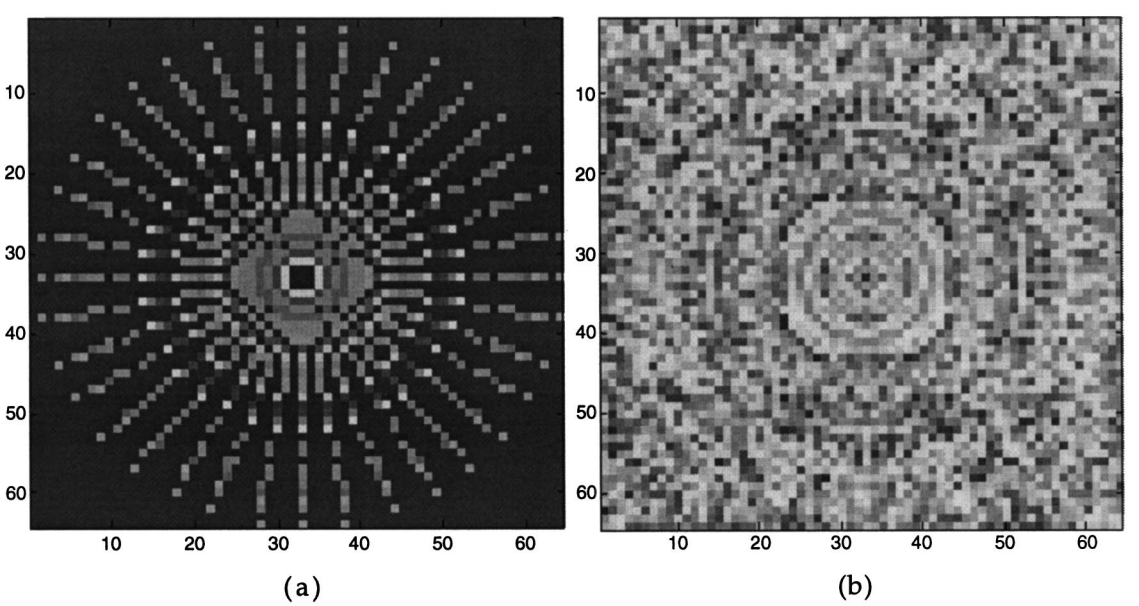

Fig. 2 (a) Ring filter transfer function and (b) ring filter impulse response.

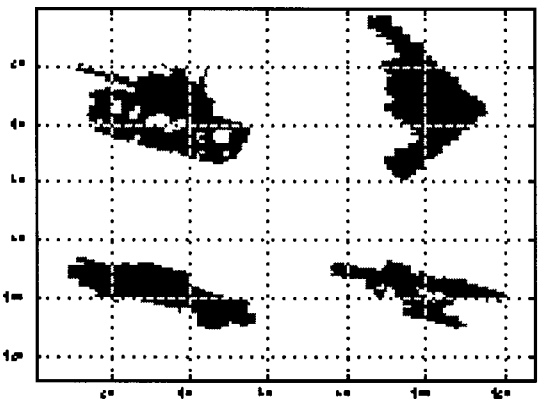

Fig. 3 Different images used in testing the filters, the target, a generic tank, and decoys—a B-2 stealth bomber, propeller plane, and a 929 Porsche.

taking a single half of a slice from the FT of the 0-deg rotated image and repeating it at incremental angles about the center of the Fourier plane to approximate the transfer function of the ring filter given in Eq. (2). Note that if we were to implement the filter by means of Eq. (1), we would require infinitely thin lines for each slice. Since the actual slices have definite thicknesses, we must approximate the filter transfer function by using a finite number of half slices. In this example, we have chosen to repeat the half slice of choice 36 times, hence this half slice is repeated at incremental angles of $(2\pi)/36$. The choice for the half-slice used in the example here was made arbitrarily and could perhaps be improved if optimization algorithms were used for its selection. We discuss this further in the conclusions section of the paper.

To test the discrimination ability of the ring filter we use the input scene shown in Fig. 3. We do not optimize the filter, nor do we try to show an absolute measure of how well the filter discriminates alike objects. We observe the recognition capability of this filter relative to other filters, namely, the SDF and the MF. Hence, any set of targets can be used.

The ring filter is an invariant filter for the entire 360-deg rotations of the target. Due to symmetry, however, it is only necessary to test a 180-deg range of the distortion. To show the relative performance of the ring filter we require some metrics. Established metrics for the performance are the peak correlation (PC) and the peak correlation energy[8–10] (PCE) as well as a metric that measures the ratio of the relative average mean of the target to the relative variance. This metric has been established in the literature and is referred to as the Fisher discriminant measure[11,12] (FDM). Figure 4 shows the correlation results of the MF, SDF filter, and the ring filter when the input is the 20-deg rotated images shown in Fig. 3.

These results show that for a particular distorted scene and 20-deg in-plane rotation, the ring filter, which uses only a single half slice of information from a single training image produces a larger relative target correlation peak than the MF or the SDF filter. Figure 5 presents the PC intensity and the PCE results for other input scenes in the distortion range. The data in Fig. 5 are provided at every 5-deg in-plane rotation increment of the image, starting

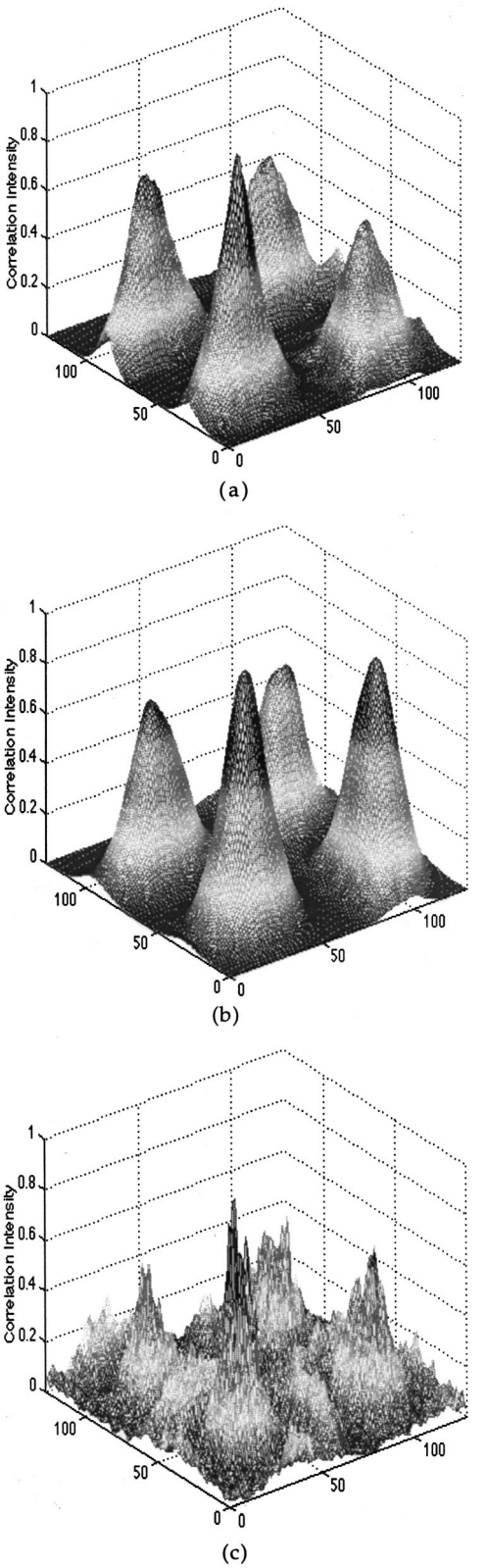

Fig. 4 Correlation results of (a) the MF, (b) the SDF filter, and (c) the ring filter with 20-deg in-plane rotated input objects.

with the 0-deg input and ending with the 180-deg in-plane rotated input. Having an invariant filter implies that the filter response remains constant as distortion is increased; i.e., we would like the ring filter to find the target and then

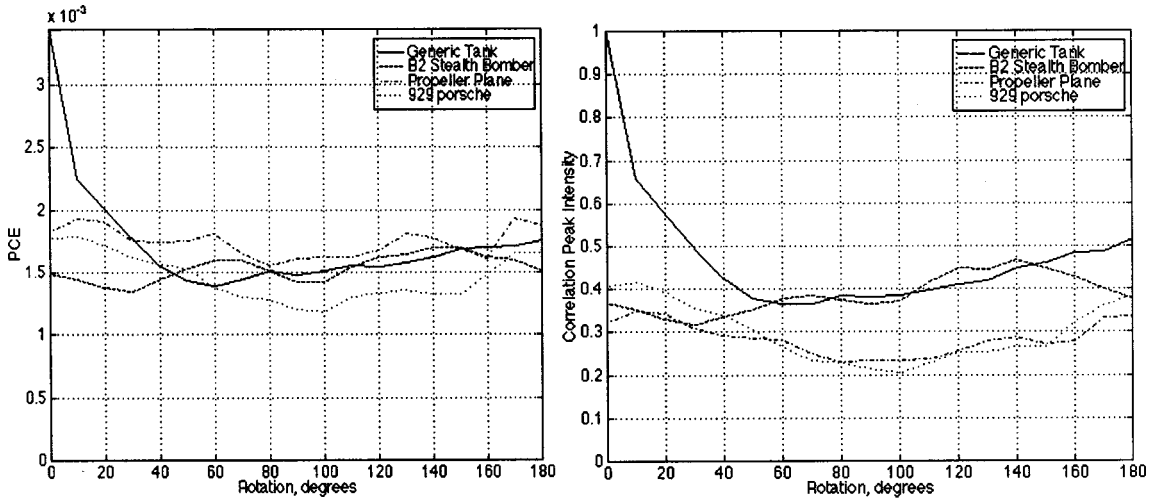

(a)

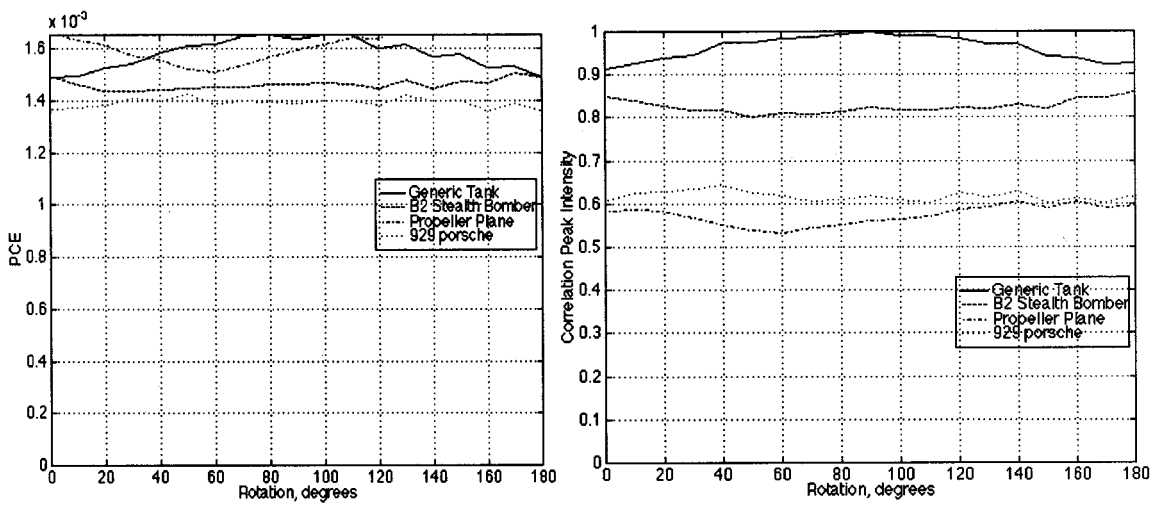

(b)

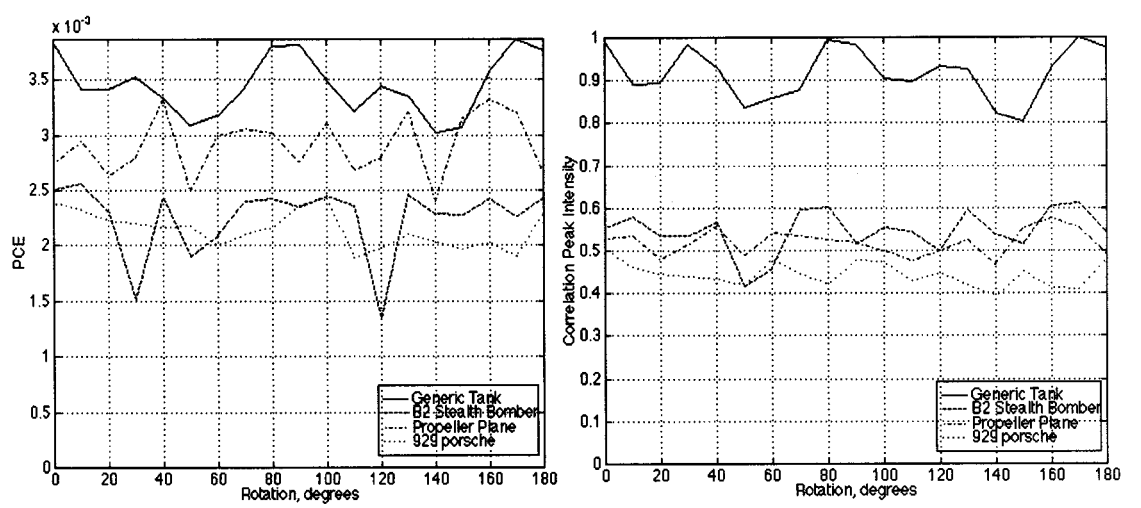

(c)

Fig. 5 PC and the PCE results of the cross-correlations of the rotated objects with (a) the matched filter, (b) the SDF filter, and (c) the ring filter.

Table 1 The FDM used to evaluate the discrimination performance of each of the filters under consideration.

FDM	Match Filter	SDF Filter	PSDF Filter
PC	1.1	5.7	23.3
PCE	0.1	0.5	4.1

maintain an invariant response to the distortion. Figure 5 shows that the ring filter is capable of clearly discriminating between the target and the other objects [Fig. 5(c)], and have a relatively flat response across the distortion range, where the relativity is in reference to the SDF and the MF. Peak target correlation value relative to the peak false target correlation value for the ring filter is $\sim$1.6 and the minimum target correlation peak to the maximum false target correlation peak is $\sim$1.3. This implies a fair discrimination capability. These same measurements for the SDF filter are $\sim$1.17 and 1.05, which are significantly lower than those of the ring filter, and for the MF they are $\sim$2.0 and 0.08, which indicate a large variation in the distortion range of the target.

The FDM was used in conjunction with the PC and the PCE to calculate the discrimination performance of the projection SDF (PSDF) filter relative to the SDF and the MF. The FDM can be given by

$$\mathrm{FDM}_{\mathrm{PC}}=\frac{(\eta_{\mathrm{PC}_T}-\eta_{\mathrm{FT}})^2}{\sigma^2_{\mathrm{PC}_T}+\sigma^2_{\mathrm{PC}_{\mathrm{FT}}}}, \tag{11}$$

where $\mathrm{FDM}_{\mathrm{PC}}$ refers to the FDM relative to the PC results, η_{PC_T} denotes the mean for the target (tank) PC values, $\eta_{\mathrm{PC}_{\mathrm{FT}}}$ refers to the mean for the false targets (the 929 Porsche, propeller plane, bomber plane) PC values, $\sigma^2_{\mathrm{PC}_T}$ is the variance of the target PC values, and $\sigma^2_{\mathrm{PC}_{\mathrm{FT}}}$ is the variance for the false target PC metric throughout the entire distortion range. The use of these equations with the PCE metric is denoted by replacing the PC subscript with a PCE subscript. In the best-case scenario, the mean value for the false targets would be zero and the target mean value would be very large, the peak values for the target would remain constant across the distortion range, and the standard deviation would thus be zero. Hence Eq. (11) leads to a very large number for the best performance of the filter. The results of these tests are presented in Table 1. The Fisher measure shows that the PSDF filter has outperformed the other filters in discrimination simulations performed here.

3 Conclusions and Future Research

We have introduced an SDF rotationally invariant filter, developed its theoretical basis, and related this to the well-known PST. The simulation efforts shown here utilized the PC, PCE, and the FDM to evaluate the ring filter performance relative to the two benchmark filters used here, the MF and the SDF filter. These metrics show that the ring filter is capable of significantly outperforming the MF and the SDF without any special optimization procedures. Other procedures can be utilized to optimize the performance of the ring filter. These include the exploration of the utility of the different powers of $|\omega|$ [Eq. (2)] or the utilization of other 1-D filtering algorithms which could pull out unique features of the target prior to their combination via the PST. The use of interpolation schemes is yet another method that could be explored to improve performance of the ring filter. An optimization process could also be devised to look at the spacing in angle between repeated half slices to minimize the peak correlation variation and information overlap. These topics remain as possible areas for future work.

References

1. H. Stark and P. Indraneel, ''An investigation of computerized tomography by direct Fourier inversion and optimum interpolation,'' *IEEE Trans. Biomed. Eng.* **BME-28**(7), 496–505 (1981).
2. R. N. Bracewell, ''Strip integration in radio astronomy,'' *Aust. J. Phys.* **9**, 198–217 (1956).
3. D. Dudgeon and R. M. Mersereau, *Multidimensional Digital Signal Processing*, Prentice-Hall, Englewood Cliffs, NJ (1984).
4. V. R. Riasati and M. A. G. Abushagur, ''Projection-slice synthetic discriminant functions for optical pattern recognition,'' *Appl. Opt.* **36**(14), 3022–3034 (1997).
5. V. R. Riasati, M. A. G. Abushagur, and D. Gregory, ''Phase-only projection-slice synthetic discriminant functions for invariant optical pattern recognition,'' *Proc. SPIE* **3073**, 76–86 (Apr. 1997).
6. V. R. Riasati, ''Projection-slice synthetic discriminant functions for pattern recognition,'' PhD Dissertation, Electrical and Computer Engineering Department, University of Alabama in Huntsville (Apr. 1996).
7. A. D. Poularikas, *The Transforms and Applications Handbook*, CRC Press, IEE Press, Boca Raton, FL (1996).
8. J. L. Horner, ''Metrics for assessing pattern-recognition performance,'' *Appl. Opt.* **31**, 165–166 (1992).
9. V. B. V. K. Kumar and L. Hassebrook, ''Performance measures for correlation filters,'' *Appl. Opt.* **29**(20), 2997–3006 (1990).
10. J. L. Horner, Ed., *Optical Signal Processing*, Academic Press, New York (1987).
11. D. Casasent, *Optical Signal Processing* J. H. Horner, Ed., Academic Press Inc., Orlando FL (1987).
12. K. Fukunaga, *Interdiction to Statistical Pattern Recognition*, Academic Press, Boston (1990).

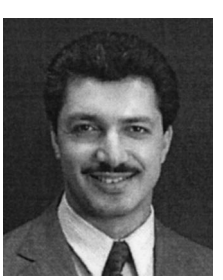

Vahid R. Riasati received his BSEE, MSEE, and PhD degrees in electrical and computer engineering from the University of Alabama in Huntsville in 1986, 1989, and 1996, respectively. He was with the Center for Applied Optics from 1987 to 1988 in the atmospheric optics area. From 1988 to 1993, he worked for the defense industry, where he developed signal processing algorithms and simulation tools for sensor systems and acousto-optical (AO) signal processor systems and designed and implemented breadboard range-Doppler AO systems. He worked toward his doctoral degree from 1993 to 1996 in optical pattern recognition, and was a visiting assistant professor with the University of Alabama in Huntsville from 1996 to 1998, where he conducted research in the area of microcavity coupling systems and optical pattern recognition. Dr. Riasati became an assistant professor with the University of South Alabama in 1998 and he is currently performing research in image processing and optical pattern recognition. He is a member of SPIE, OSA, and IEEE.

Partha P. Banerjee is a professor of electrical and computer engineering with the University of Alabama in Huntsville. He received his B Tech degree in electronics and electrical communication engineering from the Indian Institute of Technology, Kharagpur, in 1979 and his MS and PhD degrees in electrical and computer engineering from the University of Iowa, Iowa City, in 1980 and 1983, respectively. Professor Banerjee is the author or coauthor of over 150 professional papers and is a fellow of the OSA and SPIE and a senior member of the IEEE.

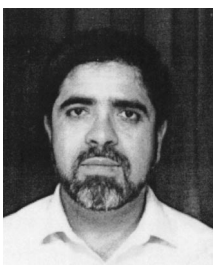

Mustafa A. G. Abushagur received his BSEE degree from Tripoli University and his MSc and PhD degrees from the California Institute of Technology, all in electrical engineering. He was an assistant professor with the University of Rochester, and in January 1985 he joined the faculty of the University of Alabama in Huntsville, where he is currently a professor of electrical and computer engineering and optical science and engineering. His research interests include optical signal processing and computing, optical fiber communication and sensors, and diffraction and the scattering theory of light. He has published more than 80 papers and five invited book chapters and has edited a book. He is a senior member of the IEEE and a member of the OSA and SPIE.

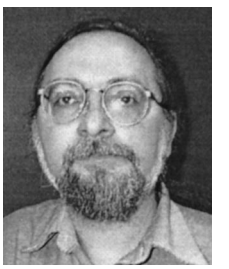

Kenneth B. Howell received his BS degrees in mathematics and physics from Rose-Hulman Institute of Technology in 1973 and his PhD in mathematics from Indiana University in 1978 under the direction of Dr. M. Lowengrub. He is currently an associate professor in the Department of Mathematical Sciences at the University of Alabama in Huntsville. In addition to his academic research leading to papers in elastostatics, generalized functions, and Fourier analysis, Dr. Howell has done industrial research in such diverse areas as quantum optics, holography, systems performance, and resource allocation.